



# Research on Settlement Analysis and Calculation of Taxiway Bridge

Ai Li \*, Yonggang Yang

Civil Aviation University of China, China Service Building, Chaoyang District, Beijing, China

\*E-mail: mahogany@126.com

**Abstract.** This article uses FLAC<sup>3D</sup> 7.0 software to simulate, calculate, and analyze the settlement of a taxiway bridge. The boundary conditions are set as free field boundary and static boundary, and the Burgers-Mohr model is selected as the constitutive model. The Class IV and V loads of the taxiway bridge are equivalent to two types of half sine waves. Based on historical records and actual observation values, the load of the taxiway bridge is loaded through the mapping relationship between the number of periods of the half sine waves and time. The settlement data of the taxiway bridge in December 2024, simulated and calculated using the Burgers-Mohr model, is 27.56 cm, which is basically consistent with the actual situation. By December 2035, the simulated calculation will still result in an additional settlement of 5.98 cm, which may have exceeded the standard limit in practice. Certain measures need to be taken to alleviate the settlement rate. FLAC<sup>3D</sup> 7.0 was used to simulate and calculate the settlement of the taxiway bridge at different groundwater levels. The settlement amplitude in the dry season of 2024 and 2035 was 2.76 cm and 3.36 cm larger than that in the wet season of the same year, which is basically consistent with the engineering estimation. Although precipitation wells can alleviate the leakage problem of taxiway bridge foundations, in addition to high operating and maintenance costs, they can cause additional settlement of the taxiway bridge, and there is a certain coupling effect between settlement and leakage. Therefore, it should be used with caution when the groundwater level is low, with limited auxiliary use when the groundwater level is high, and gradually reduced in use as the settlement amplitude of the taxiway bridge increases.

**Keywords:** taxiway bridge, frame, settlement, FLAC, Burgers-Mohr

## 1 Introduction

Most of the existing taxiway bridges in China use reinforced concrete and prestressed concrete materials, and the structural forms mainly include beam bridges, rigid frame bridges, and closed frame bridges<sup>[1]</sup>. The three structural forms account for about 47%, 23%, and 30% respectively<sup>[2]</sup>. Closed frame bridges are often used to solve the intersection problem between taxiways and existing highways, which can maximize the impact on the normal taxiing of aircraft. Prefabricated box culverts are used for segmented

top-down construction. As a key facility in transportation hubs such as airports and ports, closed frame taxiway bridges are prone to leakage and settlement due to long-term effects of dynamic loads, environmental erosion, and changes in groundwater levels, which can reduce their service life and even threaten structural safety.

When the foundation of a frame bridge settles unevenly, additional internal forces will be generated, increasing the risk of structural damage to the frame bridge. When the foundation is uniformly settled, it is generally believed that uniform settlement has little impact on the frame bridge as it generally does not generate additional internal forces. But when the settlement amplitude is large and the groundwater level is shallow, it will cause water accumulation in the foundation of the frame bridge, leading to steel reinforcement corrosion, decreased steel-concrete strength, and reduced structural durability and service life.

The research on the settlement of frame bridge foundations mainly focuses on the impact of construction on existing frame bridges and the monitoring of frame bridge settlement. Wang, J.<sup>[3]</sup> et al. conducted research on the deformation law and control measures of shield tunneling under railway frame bridges, and pointed out that excavation under shield tunneling can cause settlement at the top of the tunnel, but the structural settlement deformation of railway frame bridges is relatively small. Tang, X.<sup>[4]</sup> et al. studied the deformation and dynamic response of subway shield tunneling through existing railway frame bridges, and calculated that the maximum track settlement after the left line of the shield tunneling was excavated first was 3.0mm. Li, H.<sup>[5]</sup> conducted research on the settlement mechanism and control technology of shield tunneling through existing high-speed railway frame bridges, and analyzed and summarized the time history law of settlement at the edge position of the frame bridge with the subway excavation process. Yuan, G.<sup>[6]</sup> conducted research on the monitoring and evaluation of settlement and safety status of composite frame bridges. Based on numerical simulation research results and combined with relevant engineering safety evaluation methods, a safety status evaluation model for composite frame bridges in coal mining subsidence areas was established. As an important type of taxiway bridge, there are few studies on the settlement of closed frame taxiway bridges.

In engineering practice, the natural settlement of foundations is generally achieved using the layered summation method, and the settlement under load is achieved by adjusting the values of  $\alpha_i$  and  $\alpha_{i-1}$ . Some literature has proposed settlement calculation methods for loess and cohesive soil foundations, which have enriched our understanding of the characteristics of loess and cohesive soil. However, the research on settlement caused by aircraft loads on taxiway bridges and corresponding water rich soil creep is not sufficient.

## 2 Parameters and Status of the Taxiway Bridge

The closed frame taxiway bridge (hereinafter referred to as the "taxiway bridge") studied in this article was completed on March 20, 1994. The bridge is 25.80 meters wide and the box culvert is 60.00 meters long. Non motorized vehicle lanes are set up on both sides of the bridge, with each lane being about 3.50 meters wide and a net height

of 2.60 meters. There is a motorized vehicle lane between the two non motorized vehicle lanes, with a total width of about 17.80 meters and divided into two spans, with a span of 8.65 meters and a net height of 4.50 meters. When completed, the bridge top elevation was about 33.30-33.50 meters, the non motorized vehicle lane elevation on the inside of the bridge was about 29.10-29.80 meters, and the motorized vehicle lane elevation was about 27.20-27.70 meters. It can be seen that the bridge top is about 3.70-4.20 meters higher than the non motorized vehicle lane, and the bridge top is about 5.80-6.20 meters higher than the motorized vehicle lane. The height of the non motorized vehicle lane is about 1.90-2.10 meters higher than that of the motorized vehicle lane, and the design load of the box culvert is 500 tons. There is a water collection tank under the southern road surface, which is about 2.60 meters lower than the road surface and has a volume of 270 cubic meters.

Freight North Road is located in the western area of the Capital Airport and was built in 1994. The road starts from the freight road in the south and ends at the airport north line in the north, with a total length of about 2.9 kilometers. It is a second-class highway as a trunk road. The road partially passes through the airfield, with a total of 5 taxiway bridges and 4 airside roads crossing over the North Freight Road. The location of the taxiway bridge is at the low point of the Capital Airport area, which is prone to groundwater seepage and rainwater drainage problems.

The estimated compressive strength of bridge pier concrete is 56.1 MPa~59.4 MPa. The maximum carbonization depth of the west bridge pier is 7.50 mm, and the maximum carbonization depth of the east bridge pier is 8.00 mm. Based on the analysis of the thickness test results of the steel reinforcement protective layer, carbonization has not yet affected the steel reinforcement. The thickness of the steel protection layer for the longitudinal main reinforcement of the bridge pier is mainly distributed between 34 mm and 45 mm, with a spacing of 80 mm to 120 mm between the steel bars. There are no obvious defects in the concrete of the bridge piers on both sides of the taxiway bridge, and there are 23 defective areas in the side ditches next to the bridge piers. After on-site verification, it was determined to be a water rich area.

The elevations of the four corners of the taxiway bridge are 27.030 m, 27.018 m, 27.403 m, and 27.417 m, respectively. (December 2024). The corresponding corner elevations on the completion drawing are 27.30 m, 27.30 m, 27.70 m, and 27.70 m (March 1994). The settlement of the four corner points has reached 27.0 cm, 28.2 cm, 29.7 cm, and 28.3 cm respectively (December 2024), and the settlement is basically uniform, but it is close to the upper limit of 30 cm allowed for the settlement of Class II highway bridges as stipulated in the "Code for Design of Highway Roadbeds"<sup>[7]</sup>.

### 3 Setting of FLAC<sup>3D</sup> 7.0 Finite Difference Calculation

#### 3.1 Burgers-Mohr Model

Creep refers to the phenomenon of deformation increasing over time after being subjected to external forces. The area where the sliding bridge is located is mainly composed of silt and cohesive soil. The academic community has conducted extensive research on the creep characteristics of cohesive soils, such as Ma, Y.<sup>[8]</sup> et al. who studied

the creep characteristics of anchor rods in cohesive soils in the Beijing area. Lu, P.<sup>[9]</sup> conducted a study on the creep characteristics of saturated soft clay. For a long time, it has been widely believed that the deformation of loess is instantaneous, and its creep characteristics have been ignored. As scholars gradually discover in engineering practice that non cohesive soils also undergo creep deformation. Zhu, J.<sup>[10]</sup> et al. conducted experimental research on the comparison of consolidation creep characteristics between silt and loess, while Chen, L.<sup>[11]</sup> studied the typical creep characteristics of loess and its multi factor influence laws. The combination of saturated silt and cohesive soil can be classified as soft soil.

The Burgers-Mohr model in FLAC<sup>3D</sup> 7.0 is also a constitutive model that combines Burgers viscoelastic creep model and Mohr Coulomb plastic criterion, used to describe the time-dependent creep behavior and elastic-plastic yield characteristics of materials such as soil. This model is suitable for long-term stability analysis. Through the Burgers Mohr model, FLAC<sup>3D</sup> 7.0 can more accurately reflect the viscoelastic plastic behavior of materials under long-term loads, providing a key basis for long-term stability assessment of engineering.

### 3.2 Boundary Condition

In FLAC<sup>3D</sup> 7.0, Free Field Boundary and Static Boundary are two commonly used boundary condition setting methods, suitable for dynamic analysis and static analysis, respectively. By selecting appropriate free field or static boundaries, the accuracy and efficiency of FLAC<sup>3D</sup> 7.0 simulation can be significantly improved.

The free field boundary is used to simulate infinite or semi infinite domains, avoiding the reflection of wave energy at the model boundary and ensuring the accuracy of dynamic analysis. The free field boundary is achieved through the coupling of viscous boundary and free field mesh. The viscous boundary exerts a resistive force on the model boundary, absorbing the energy of the incident wave and preventing reflection. A free field grid is set on the outside of the model to simulate the free field motion in an infinite domain (natural waves without structural disturbances). The lateral boundaries of the main grid are coupled with the free field grid through dampers, and the unbalanced force of the main grid is applied through the free field grid.

Static boundaries are used to limit the rigid body displacement of the model in static analysis, ensuring numerical stability. Static boundaries are achieved by fixing displacement or constraining velocity. The specific method for static boundary is to set free dampers in the tangential and normal directions of the model to absorb incident waves.

### 3.3 Damping Form and Parameter Settings

FLAC<sup>3D</sup> 7.0 offers three forms of damping: Rayleigh damping, local damping, and hysteresis damping. This article uses Rayleigh damping in power calculations. Rayleigh damping can reduce the amplitude of natural vibration modes in a system, and is generally suitable for analysis of structures and elastic bodies. Rayleigh damping has two parameters, namely the minimum critical damping ratio and the minimum center

frequency. When plastic failure occurs within the FLAC<sup>3D</sup> region, the stiffness proportional damping is closed. However, mass proportional damping is still effective. If the model experiences excessive failure, the mass proportion term may suppress yielding. In the calculation model of this article, the minimum critical damping ratio is taken as 2%, the minimum center frequency is taken as 2, and mass proportional damping is used.

### 3.4 Load and Equivalent of Taxiway Bridge

#### *Characteristics of Load on Taxiway Bridge.*

##### **Long Term Nature.**

The load on taxiway bridge is a long-term cyclic process.

##### **Low Frequency.**

From the completion of the taxiway bridge in 1994 to 2008, the number of flights taking off and landing at the Capital Airport experienced a rapid growth, from about 180,000 to about 580,000, and then remained at about 580,000 until 2019. After the completion of the Beijing Daxing International Airport, the impact of diversion and the COVID-19 epidemic rapidly decreased to about 290,000 in 2020, and then recovered to 420,000 in 2024. It is expected that the number will gradually recover to 500,000 in the next decade.

Based on the actual observation of the taxiway bridge and some archival data from the Capital Airport, the average daily frequency of aircraft crossing the bridge by year is shown in Table 1. The load of taxiway bridge has low-frequency characteristics, with only 11-32 aircraft crossing every 24 hours, which is significantly different from highway bridges.

**Table 1.** Average hourly frequency of aircraft crossing taxiway bridge by year.

| Year | Average Daily Frequency | Year | Average Daily Frequency | Year             | Average Daily Frequency |
|------|-------------------------|------|-------------------------|------------------|-------------------------|
| 1994 | 11                      | 2008 | 31                      | 2022             | 16                      |
| 1995 | 11                      | 2009 | 30                      | 2023             | 20                      |
| 1996 | 12                      | 2010 | 31                      | 2024             | 21                      |
| 1997 | 14                      | 2011 | 31                      | 2025 (predicted) | 22                      |
| 1998 | 16                      | 2012 | 31                      | 2026 (predicted) | 22                      |
| 1999 | 18                      | 2013 | 31                      | 2027 (predicted) | 23                      |
| 2000 | 19                      | 2014 | 32                      | 2028 (predicted) | 24                      |
| 2001 | 20                      | 2015 | 32                      | 2029 (predicted) | 24                      |
| 2002 | 21                      | 2016 | 32                      | 2030 (predicted) | 24                      |

|      |    |      |    |                  |    |
|------|----|------|----|------------------|----|
| 2003 | 22 | 2017 | 32 | 2031 (predicted) | 25 |
| 2004 | 24 | 2018 | 32 | 2032 (predicted) | 25 |
| 2005 | 25 | 2019 | 32 | 2033 (predicted) | 25 |
| 2006 | 26 | 2020 | 16 | 2034 (predicted) | 26 |
| 2007 | 26 | 2021 | 16 | 2035 (predicted) | 26 |

**Instantaneousness.**

The time for the plane to cross the bridge is very short, only lasting for more than two seconds. For a certain point on the bridge deck, the duration is even shorter, with the characteristic of instantaneous load.

**Vibration.**

Due to its inherent vibration, airplanes can cause vibration on bridge decks, and the two types of vibration will couple with each other<sup>[12]</sup>, causing vibration in nearby soil and resulting in viscoelastic viscoplastic deformation of the soil.

**Load on Taxiway Bridge.**

The maximum load of this taxiway bridge is a Class V load model, namely B777-300ER, with a total weight of 3,525 kN. The main landing gear has three axles with an axle load of 1,115 kN, and there is one front landing gear with an axle load of 180 kN<sup>[1]</sup>. Another one is the Type IV load model, namely B747-400, with a total weight of 3,990 kN. The main landing gear has four axles with an axle load of 950 kN<sup>[1]</sup>.

**Equivalent of Load.** Due to the above characteristics, the settlement of taxiway bridge can be seen as a function of the number of times an aircraft crosses the bridge. And the load of a single aircraft crossing the bridge is equivalent to a half sine wave, which is represented by formula (1).

$$F(t) = F_0 \sin(2\pi ft) \quad t \in [0, t_0] \tag{1}$$

$t_0$  is the time for the aircraft to pass through the taxiway bridge,  $F_0$  is the equivalent amplitude of the load, and is calculated using equation (2).  $f$  is the frequency related to the bridge span, calculated using equation (3).

$$F_0 = DAF \times P \tag{2}$$

$DAF$  is the dynamic amplification factor, which is taken as 1.4 in this article, and  $P$  is the uniaxial standard load.

$$f = \frac{v}{2L} (Hz) \tag{3}$$

$v$  is the taxiing speed of the aircraft, based on actual observation data, the average speed of the aircraft passing through the taxiway bridge is taken as 36 km/h, and  $L$  is the span of the taxiway bridge.

By using the above method, the load on the taxiway bridge can be equivalent to a function of the number of times the aircraft crosses the bridge.

## 4 Establishment of Numerical Calculation Model

### 4.1 Constitutive Model and Initial Stress Field

The soil thickness is taken as 35 meters, the width is taken as 60 meters, and the length is taken as 75 meters. According to the internal geological survey data of the Capital Airport, the depth of backfill soil is 4.2 meters, and the groundwater level during the wet season is taken as -3 meters. The backfill soil is divided into 5 layers below, and the soil parameters are shown in Table 2. The setting of deep soil below 15 meters is the same as the fifth layer. Poisson's ratio  $\nu_{ur}$  is set to 0.28. The constitutive model is selected as the Burgers Mohr model. The initial geostress field of the model is shown in Figure 1.

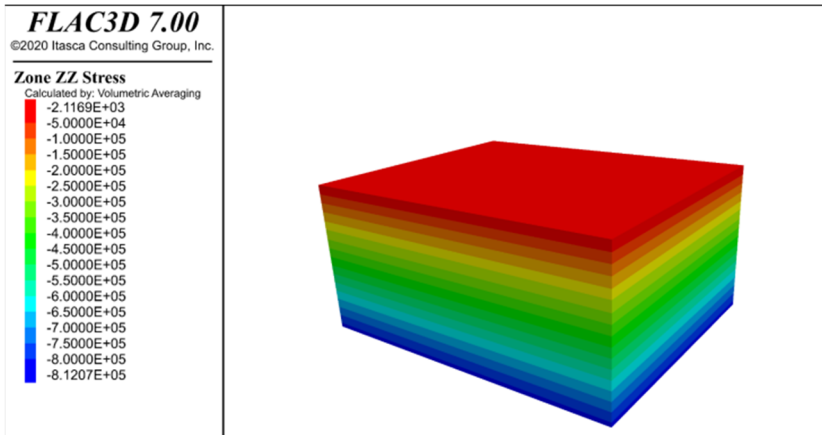


Fig. 1. Initial ground stress field.

Table 2. Parameter setting of soil mass.

| Layer No. | Layer Name    | Thick-ness/m | Unit Weight/<br>kN·m <sup>-3</sup> | Floating Weight/<br>kN·m <sup>-3</sup> |
|-----------|---------------|--------------|------------------------------------|--|
| 1         | Silt          | 2.30         | 20.5                               | 10.8                                   |
| 2         | Cohesive soil | 1.40         | 18.6                               | 9.6                                    |
| 3         | Silt          | 1.00         | 19.7                               | 10.3                                   |
| 4         | Cohesive soil | 1.60         | 18.3                               | 8.6                                    |
| 5         | Silt          | 4.50         | 19.8                               | 10.1                                   |

| Layer No. | Layer Name    | Cohesion/<br>kPa        | Internal Friction angle/ $^{\circ}$            | Friction Resistance with Anchor Body/kPa |
|-----------|---------------|-------------------------|--|--|
| 1         | Silt          | 10.00                   | 10.00  | 50.00                                    |
| 2         | Cohesive soil | 38.00                   | 13.50  | 50.00                                    |
| 3         | Silt          | 20.00                   | 15.00  | 50.00                                    |
| 4         | Cohesive soil | 38.00                   | 13.50  | 50.00                                    |
| 5         | Silt          | 20.00                   | 15.00  | 50.00                                    |
| Layer No. | Layer Name    | Cohesion Underwater/kPa | Internal Friction Angle Underwater/ $^{\circ}$ | m in Calculation/ $MN \cdot m^{-4}$      |
| 1         | Silt          | 8.00                    | 8.00   | 2.00                                     |
| 2         | Cohesive soil | 30.00                   | 11.00  | 6.09                                     |
| 3         | Silt          | 17.00                   | 12.00  | 5.00                                     |
| 4         | Cohesive soil | 30.00                   | 12.00  | 4.00                                     |
| 5         | Silt          | 15.00                   | 10.00  | 4.00                                     |

### 4.2 Establishment of Geometric Solid Model and Mesh Division

Establish a geometric solid model on the soil according to the actual dimensions of the taxiway bridge. On this basis, the model is meshed as shown in Figure 2. The geometric solid model is divided into 213,600 grids, with a total of 229,555 nodes set.

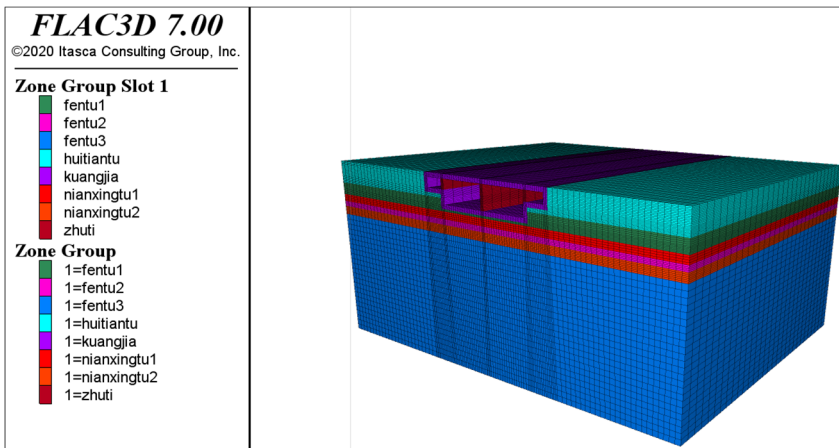


Fig. 2. Mesh division.

### 4.3 Boundary Condition Setting

Considering the absorption capacity of the sliding bridge and taxiway surface for load waves, they are set as static boundaries. In order to fully absorb load waves, the depth of the soil is relatively large, so the bottom of the soil is also set as a static boundary. The soil around the dynamic model is simulated using free field boundaries, as shown in Figure 3.

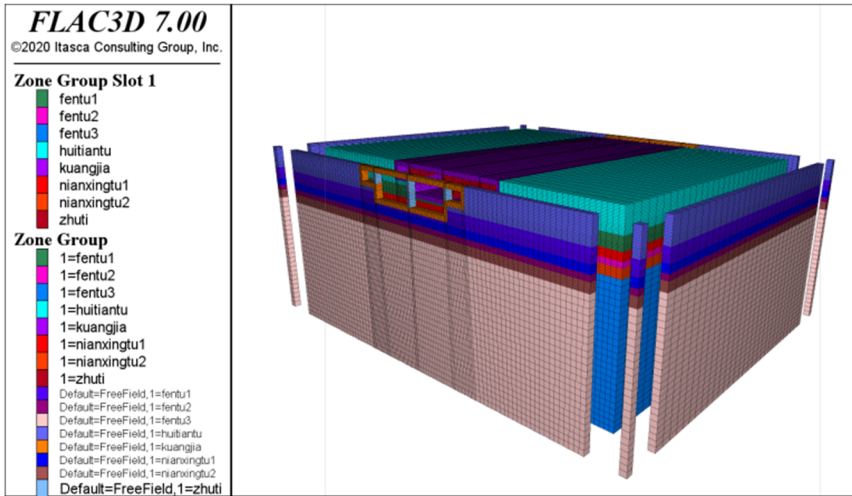


Fig. 3. Free field boundary of dynamic model.

### 4.4 Application of Load

According to actual research, the load ratio for Class IV and Class V is 2:1. From the completion of the sliding bridge in March 1994 to December 2024, a total of 177,207 cycles of IV type sine wave load and 88,605 cycles of V type load were loaded. FLAC<sup>3D</sup> 7.0 uses FISH function to express relatively regular dynamic loads. Because periodic loads belong to regular loads, this article uses the FISH function to load the load onto the top grid of the model.

## 5 Analysis of Settlement Process of Taxiway Bridge

### 5.1 Simulation of Settlement State upon Completion

The simulation calculation of the settlement state of the taxiway bridge when it was completed in 1994 is shown in Figure 4, and the vertical settlement of the motor vehicle lane is about 0.68 cm.

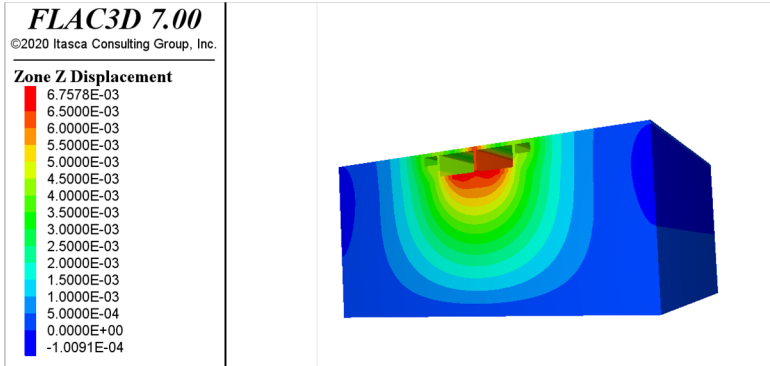


Fig. 4. Simulation of settlement state at completion.

### 5.2 Simulation of Settlement Status in December 2024

The simulation calculation of the settlement state of the taxiway bridge in December 2024 is shown in Figure 5. The settlement of the visible motor vehicle lane reached 27.56 cm, which is basically consistent with the actual situation. It can be seen that using FLAC<sup>3D</sup> 7.0 to simulate and calculate the settlement of the taxiway bridge has high practicality and reference value.

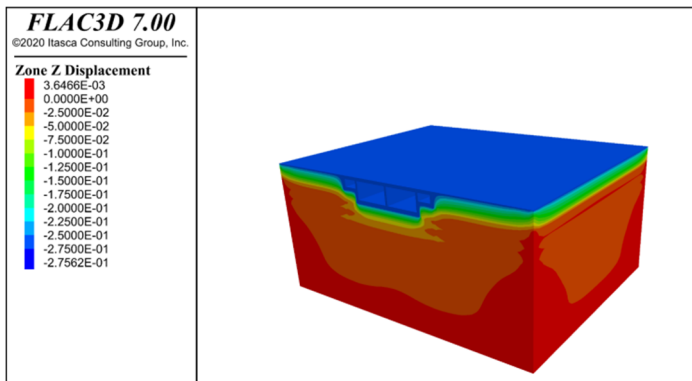


Fig. 5. Settlement simulation of taxiway bridge in December 2024.

### 5.3 Prediction of Future Settlement

Continue to increase the number of cycles for the load on the taxiway bridge, so that the number of cycles for Class IV load reaches 241,934 and the number of cycles for Class V load reaches 120,968, to simulate the settlement state of the taxiway bridge in December 2035, as shown in Figure 6. It can be seen that the settlement of the motor vehicle lane on the taxiway bridge has reached 33.54 cm, which is higher than the 5.98 cm settlement that occurred in December 2024. It is speculated that the actual settlement of the taxiway bridge at that time may exceed 30 cm.

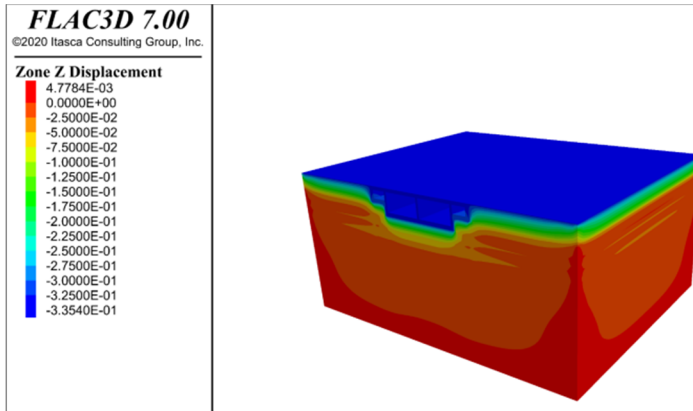


Fig. 6. Settlement simulation of taxiway bridge in December 2035.

#### 5.4 Influence of Extreme Precipitation and Freeze-thaw Cycles on Groundwater and Soil Parameters

Precipitation is an important source of groundwater recharge, but there is a lag in the image of precipitation on the groundwater level. Extreme heavy rainfall often occurs in summer in Beijing, but persistent heavy rainfall takes a long time to cause a significant rise in the groundwater level, while short-term rainstorm has limited supply due to the rapid loss of surface runoff, so heavy rainfall has little impact on the groundwater level. Hydrological data in Beijing shows that the annual water level is cyclical, with the low value of groundwater level around June each year, and the high value of groundwater level around December. Extreme rainstorm will increase the water content of surface soil, reduce the matric suction, and cause soil softening. However, the location of the sliding bridge in this article is relatively low, and the soil is in a state of water saturation and softening all year round. The road surface under the bridge has long-term water seepage, especially during the high water season when groundwater seepage is severe. Therefore, short-term heavy rainfall will not cause further increase in surface soil moisture content, and therefore has little impact on soil parameters.

The highest daytime temperature in Beijing during winter is often above 0 degrees Celsius, and the lowest nighttime temperature is often below 0 degrees Celsius. Moreover, winter is the season of abundant soil moisture, and there is a significant freeze-thaw cycle effect. Freezing soil can form an ice layer of shallow groundwater, blocking surface water infiltration. Melting soil can increase soil moisture content in the short term, which may cause small fluctuations in groundwater levels, but the overall impression of groundwater levels is not significant.

The freezing of soil can cause swelling (about 8%), leading to changes in soil structure. After melting, the porosity and bearing capacity of the soil decrease. The freeze-thaw soil under long-term loads will accelerate the softening rate of the soil, forming a significant creep effect. The biggest consequence of soil freezing and thawing is the formation of frost heave cracks in the foundation of taxiway bridges, causing serious water seepage diseases in the bridge foundation. In order to effectively solve the water

seepage diseases, it is necessary to comprehensively consider the impact of settlement and adopt treatment measures that are not easy to cause additional settlement.

### 5.5 Influence of Groundwater on the Settlement

According to the archives of the Capital Airport Group, the first layer of interlayer water in the Capital Airport area has an elevation of 28.89~30.89 meters; The second layer of interlayer water has an elevation of 25.47-27.85 meters. The elevation of the foundation of the taxiway bridge is roughly at the same level as the water between the second layer. In December 2024, the measured water level elevation in the precipitation well was 26.67 meters, which belongs to the second layer interlayer water.

According to the groundwater dynamics in the plain area of Beijing announced by the Beijing Municipal Water Affairs Bureau, the annual variation characteristics of groundwater level in recent years are: the groundwater level is relatively stable from January to February; Due to factors such as low precipitation and spring irrigation, the groundwater level shows a continuous downward trend from March to June; Affected by increased precipitation recharge from July to October, the groundwater level continues to rise; The groundwater level remained basically stable from November to December, with an annual water level difference of about 2.3 meters.

Under similar geological conditions of saturated silt and clay, based on the actual engineering data calculated by Liu H.<sup>[13]</sup>, it is roughly estimated that the impact of changes in groundwater level on the elevation of the taxiway bridge is in the range of 2.2-3.3 cm.

### 5.6 Simulating the Influence of Groundwater Level on the Settlement of Taxiway Bridge using FLAC<sup>3D</sup> 7.0

The annual groundwater level difference in the plain areas of Beijing is approximately 3 meters. Therefore, only the groundwater level in Section 3 of this chapter was changed to -6 meters to simulate the groundwater level during the dry season (June). To ensure the reference value of the calculation results, other calculation conditions such as the number of load cycles were set to remain unchanged. The results are shown in Figures 7 and 8.

The settlement of the taxiway bridge reached 30.32 cm in June 2024 and is expected to reach 36.90 cm in June 2035. The settlement amplitude is 2.76 cm and 3.36 cm greater than that in December 2024 and December 2035, respectively, which is basically consistent with the engineering estimation.

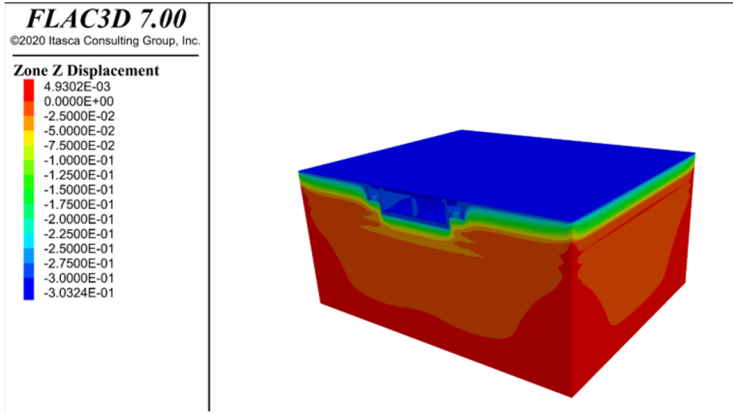


Fig. 7. Settlement simulation of taxiway bridge in June 2024.

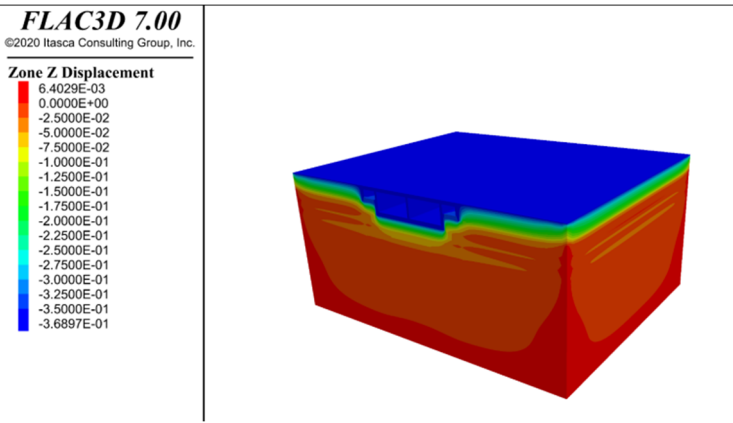


Fig. 8. Settlement simulation of taxiway bridge in June 2035.

Although precipitation wells can alleviate the leakage problem of taxiway bridge foundations, in addition to high operating and maintenance costs, they can cause additional settlement of taxiway bridge, and there is a certain coupling effect between settlement and leakage. Therefore, it should be used with caution when the groundwater level is low, with limited auxiliary use when the groundwater level is high, and gradually reduced in use as the settlement amplitude of the taxiway bridge increases. It cannot be used as the main means to solve the current leakage problem of taxiway bridge.

## 6 Conclusions

Aiming at the long-term settlement of frame taxiway bridge, this paper reveals the coupling mechanism of aircraft load and groundwater change through FLAC<sup>3D</sup> 7.0 modeling and Burgers-Mohr constitutive analysis. The model has high prediction accuracy

(simulation error <3% in 2024), which has practical reference value for engineering maintenance.

At present, the robustness of the model needs to be improved so that it can be applied to two other types of taxiway bridges with considerable accuracy. This is one of the prospects for the next step of work. In addition, due to their importance, the management of taxiway bridges requires a "one bridge, one strategy" approach, and dynamic monitoring technology can serve as an important basis for management in practical work. The use of GNSS monitoring, InSAR technology, as well as support displacement detection technologies such as laser displacement sensors and LVDT, can all provide real-time recording and early-warning of taxiway bridges.

## References

1. Civil Aviation Administration of China, "Design Guidelines for Aircraft Load Bridges at Civil Airports MH/T 5063-2023," Beijing: Civil Aviation Press of China, 2023.
2. Zhang, T., "Research on Structural State Evaluation of Aircraft Taxiway Bridges," Xi'an: Chang'an University, 2021.
3. Wang, J., La, B., Meng, X., and Yang, J., "Deformation Law and Control Measures of Shield Tunnel Underpass Railway Frame Bridge Construction," *Highway* 67, no. 3(March 2022): 373-377.
4. Tang, X., Lai, X., Liu W., and Lu S. et al., "Deformation and Dynamic Response of Subway Shield Tunneling through Existing Railway Frame Bridges," *Research on urban rail transit*, <https://link.cnki.net/urlid/31.1749.U.20250117.1959.007>.
5. Li, H., "Research on Settlement Mechanism and Control Technology of Shield Tunneling through Existing High-speed Railway Frame Bridges," Chengdu: Southwest Jiaotong University, 2017.
6. Yuan, G., "Research on Monitoring and Evaluation of Settlement and Safety Status of Composite Frame Bridges," Xuzhou: China University of Mining and Technology, 2014.
7. Ministry of Transport of the People's Republic of China, "Design Specification for Highway Roadbeds JTG D30-2015," Beijing: People's Communications Press, 2015.
8. Ma, Y., Li, D., Wang, H., "Creep characteristics of anchor rods in cohesive soil in Beijing area," *Engineering Survey* S1(2014): 731-734.
9. Lu, P., "Research on creep properties of saturated soft clay," Wuhan: Wuhan Institute of Geotechnical Mechanics, Chinese Academy of Sciences, 2008.
10. Zhu J., Chen S., Ying X., and Zhou Y. et al., "Experimental study on the comparison of consolidation creep characteristics between silt and loess," *Journal of Geotechnical Engineering* 46, no. S2(2024): 82-86.
11. Chen L., "Study on the creep characteristics of typical loess and its multi factor influence law," Kunming: Kunming University of Science and Technology, 2024.
12. Zhang Y., "Study on the Coupling Effect of Beam Grid Method Aircraft Taxiway Bridge Based on Model Correction," Tianjin: Hebei University of Technology, 2018.
13. Liu H., "Exploration of Settlement Calculation and Disease Control Measures for Highway Roadbeds - Taking the S Expressway Project as an Example," *Technology and Market* 31, no.12(December 2024): 127-131.

**Open Access** This chapter is licensed under the terms of the Creative Commons Attribution-NonCommercial 4.0 International License (<http://creativecommons.org/licenses/by-nc/4.0/>), which permits any noncommercial use, sharing, adaptation, distribution and reproduction in any medium or format, as long as you give appropriate credit to the original author(s) and the source, provide a link to the Creative Commons license and indicate if changes were made.

The images or other third party material in this chapter are included in the chapter's Creative Commons license, unless indicated otherwise in a credit line to the material. If material is not included in the chapter's Creative Commons license and your intended use is not permitted by statutory regulation or exceeds the permitted use, you will need to obtain permission directly from the copyright holder.

